NICKEL RECOVERY BY CARBOTHERMIC REDUCTION FROM SLUDGE GENERATED DURING NICKEL PRODUCTION[1]

John Bernardo Vilca Neira[2]
Dener Martins dos Santos[3]
Marcelo Breda Mourão[4]
Cyro Takano[4]

Abstract
During nickel extraction from ores by Caron process a large amount of sludges is generated. These sludges still contain an average of 0.54%Ni mainly as silicate, 0.07%Co and total iron of around 30%. This work intends to recover the contained Ni and Co from them. A composite pellets was produced with petroleum coke and using CMC (carboxi-metil-cellulose) as binder. The reduction behavior was determined by weight loss at temperatures of 1423, 1473, 1523 and 1573 K and times at each temperature of 2, 5, 15,30 and 45 minutes. The reduced pellets were analyzed by Electron Microscopy and XDS. The metallic phase of Fe-Ni presented a composition varying from 1 up to 2.2%Ni, with residual Cu and Co . The reaction fraction was around 80%. At this range of temperatures the reaction fraction was very sensitive to temperature variations. For 45 minutes the reaction fraction was 50% at 1423 K and 80% at 1573 K. It was identified 2 steps for reduction reaction. The first step up to around 10 minutes is very fast and the second step after 10 minutes is slow. The apparent activation energies determined were 86 kJ/mol and 135 kJ/mol, respectively.
Key words: Slugs; Nickel; Carbothermic reduction.

[1] *Technical contribution to the 7th Japan-Brazil Symposium on Dust Processin-Energy-Environment in Metallurgical Industries and 1st International Seminar on Self-reducing and Cold Bold Agglomeration, September 8-10 2008, São Paulo City – São Paulo State – Brazil*
[2] *Graduate Student of the Metallurgical and Materials Engineering Dept. of the University of São Paulo.*
[3] *ABM member, Dr. Eng., Pos-Doctor at Metallurgical and Materials Eng. Dept. of USP.*
[4] *ABM member. Associate Professor of the Metallurgical and Materials Engineering Dept. of the University of São Paulo.*

1 INTRODUCTION

The current technological development trends is to maximize the extraction process of raw material, in order get the maximum recovery of valued metals with less damage to environment. Presently there are many alternative processes with this purpose, like zinc recovery from steelmaking dusts (sludge).[1-5]
In the Caron process for nickel production a large amount of sludges are generated due to low nickel concentration in the ore. This sludge still contains around 0.5%Ni and is the residue after reduction and leaching of ore by ammonia solution. It is expected that most of Ni is in form of silicates, therefore presenting difficulties for recovering it.[6,10]
This study tries to understand the reduction behavior when a composite pellet with petroleum coke was exposed to high temperatures (1423, 1473, 1523 and 1573 K).[7,8,9]

2 EXPERIMENTAL

2.1 Raw Material Characterization

The chemical compositions of the slug and the petroleum coke are in the Table 1.

Table 1. Chemical compositions of the sludge and of the petroleum coke. (%)

Components	C_{FIXO}	Fe	Ni	Cu	CO	Cr	Mn	SiO_2	Al_2O_3	MgO	CaO	FeO	H_2O
sludge	------	34.1	0.66	0.13	0.07	1.82	0.67	30.1	6.83	5.83	0.55	--------	-------
Coke petroleum	90,00	-------	-------	-------	-------	-------	-------	2.3	6.7	-------	------	0.6	0.4

The chemical analysis indicated that the residue is composed mainly of iron, chromium, nickel, copper and cobalt as a reducible elements and very acid "gangue".[11]
Table 2 shows the particle size distribution of the sludge.

Table 2. Particle size distribution of the sludge.

Fraction	% mass		Content, % mass		
mm	Retained	Accu	Iron	Nickel	Oxi. Silicon
>0,297	1.5	1.5	21.3	0.71	42.3
0,297 - 0,074	24.7	26.2	23.7	0.59	41.3
0,074 - 0,044	12.8	38.9	28.7	0.61	35.2
0,044 - 0,037	7.7	46.6	30.3	0.57	33.1
0,037 - 0,020	13.3	59.9	34.5	0.72	29.3
0,020 desl	28.2	88.1	39.2	0.62	26.5
Lama	119	100	42.5	0.39	19.5
Total calc.	100		32.9	0.6	31.5

The particles are very fine, with more than 60% smaller than 44 μm.

2.2 Mineralogy of the Sludge

The sludge is mostly (~80%) composed by a complex magnesium and iron silicate which contains aluminum oxide and around 20% as iron and magnesium oxides. Nickel is distributed within these phases and almost impossible to concentrate it by physical separation processes.

2.3 Pellet Composition

The dried raw materials were composed such that carbon content was enough to reduce all the reducible oxides plus approximately 7% excess. The pellet was composed with 88%slug and 12% petroleum coke, agglomerated with 0,03% of CMC (caboxy-metil-celullose). The pellets were handmade and cured during 25 days at room temperature.

2.4 Reduction Experiments

The pellets were dried and they were submitted to temperatures of 1423, 1473, 1523, 1573 K, and at times of 2, 3, 5, 10, 15, 30, 45 minutes at each temperature**.** The thermo gravimetric system with argon atmosphere with 2L/min flow was used and the weight loss was determined**.**[12,8,9,2]
The reacted fraction (reaction fraction, Fr) was calculated using the following relation:

$$F = \frac{M_i - M_t}{M x M_i}$$

From which: F_r = reaction Fraction
M_i = Initial pellet weight (g);
M_t = Pellet's weight at instant t (g);
M = maximum weight loss.

The main reducible oxides considered were: iron, nickel, cobalt and copper.

3 RESULTS AND DISCUSSION

The reaction fraction versus time was plotted for all the tested temperatures (Figure 1-A) and figure 1-B the plot ln $(1-F_r)$ versus time which show a good fit with the first order equation ln $(1-F_r) = -kt$.[13,14,15]

From Figure 2, it is possible to derive an estimate of apparent activation energy, based on the Arrhenius expressions $k=k_o.e^{(-E/RT)}$ from which, k_o, is a constant, R, the gas constant, T, the absolute temperature and E the apparent activation energy.

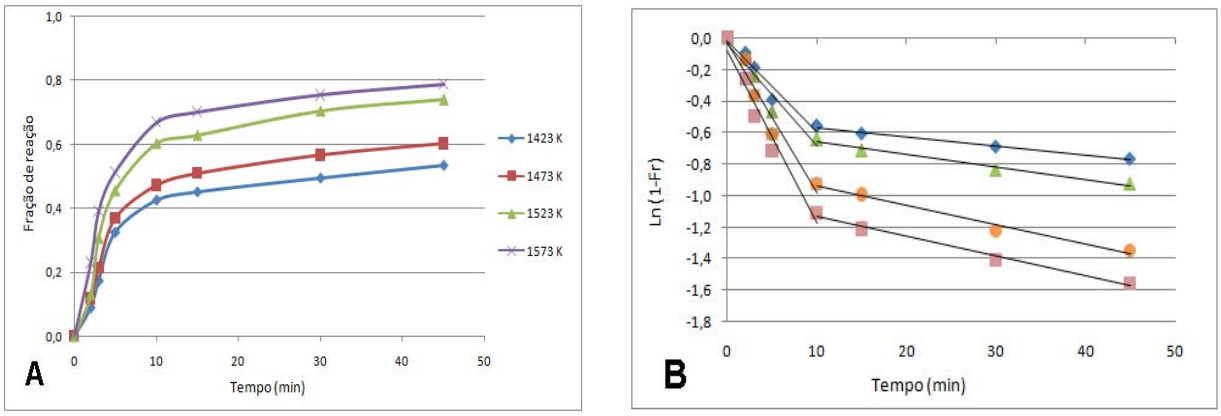

Figure 1 – Reaction Fraction versus time, (A). Ln (1-F_r) versus time, (B).

It is observed in Figure 1 that at least two different mechanisms are acting. First one with fast reaction up to around 10 minutes at temperatures and a slower reaction after that time.

The maximum reaction fraction reached at the tested conditions was 80% at 45 minutes at temperature of 1573 K

From Figure 2 the apparent activation energies were 86 kJ/mol for the initial stage up to 10 minutes and 135 kJ/mol for the stage of 10 to 45 minutes.

These results obtained show that in the beginning the reaction is probably controlled by heat transfer. The higher activation energy for times longer than 10 minutes is credited to be controlled by diffusion in the solid state. It should be noticed that this value of apparent activation energy is much lower than the one from the Boudouard reaction, which usually plays the decisive role in the control of the carbothermical reduction.

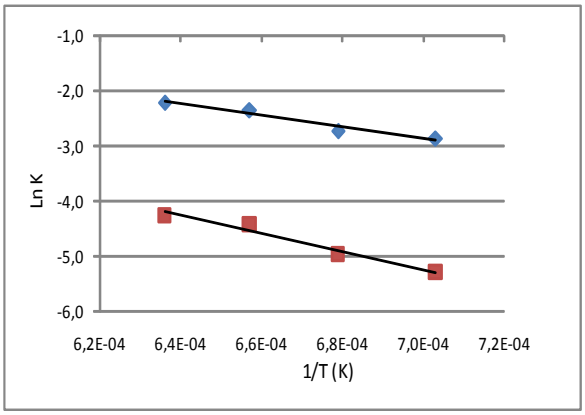

Figure 2 – Ln k versus 1/T allow us to calculate the apparent activation energy

3.1 Micrographics Analyses

Figure 3 to 6 show the results of reaction products through electronic scanning microscopy. Figure 3 shows the pellet after 5 minutes reduction at a temperature of 1423K (Figure 3A) and 1473K (Figure 3B).

It was observed in the Figure 3A the presence of three different phases in the analysis through EDS. Spot B has a high metallic content and the spot A is composed mainly by oxygen, silicon, magnesium and iron which is probably an original sludge. The third phase (black one) is the resin used for preparation of the sample. Table 3 gives the rough composition of phases A and B, by EDS. Figure 3-B

show the partially reduced pellet after 5 minutes at 1473K.. At high temperature (1473) it can be verified a higher reduction with presence of more homogeneous metallic phase. Table 4 gives the approximate compositions of different phase shown in the Figure3-B.The reaction fractions in both were around 35%.

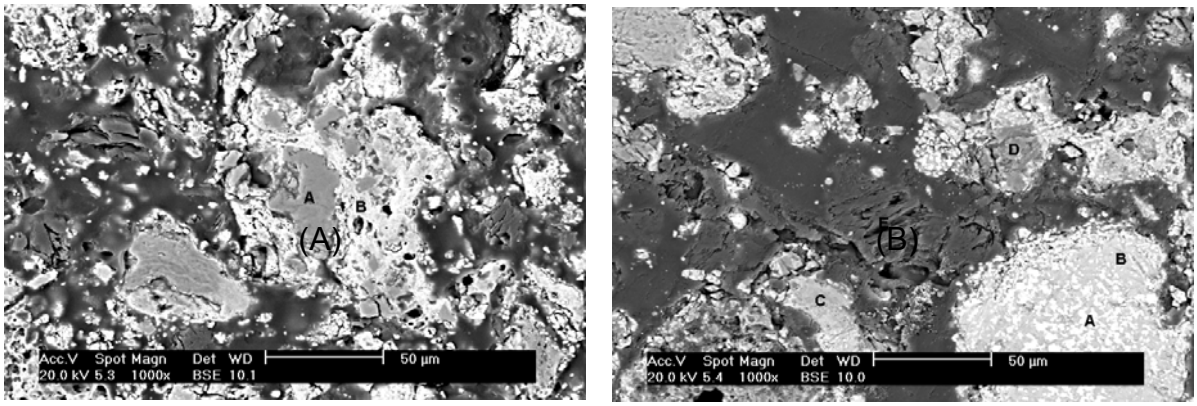

Figure 3 – Micrograph (SEM) of the self-reducing pellets submitted during 5 minutes at 1423K (A) and at 1473 (B). Reaction fractions around 35%.

Table 3. EDX of Figure 3-A

Phase	O	Mg	Al	Si	P	S	Ca	Cr	Mn	Fe	Co	Ni	Cu	Zn
A	13.57	0.00	0.43	78.75	1.86	0.85	0.13	0.42	0.22	2.79	0.27	0.43	0.50	0.19
B	5.89	1.40	9.59	16.40	1.54	0.84	0.63	1.76	1.75	56.73	1.33	0.86	0.63	0.65

Table 4 . EDX of Figure 3-B

Phase	O	C	Mg	Al	Si	P	S	Ca	Cr	Mn	Fe	Co	Ni	Cu
A	0.00	9.11	0.39	0.41	1.21	0.71	0.37	0.00	0.25	0.38	84.04	1.62	0.98	0.53
B	10.23	10.52	1.64	1.63	15.08	0.88	0.59	0.34	0.56	1.25	54.81	1.74	0.27	0.46
C	14.20	13.03	10.17	3.33	20.39	0.93	0.37	0.26	0.45	1.15	33.75	0.96	0.53	0.48
D	22.51	0.00	1.16	1.30	53.55	1.29	0.46	0.31	0.29	1.16	16.71	0.62	0.19	0.45
E	0.00	90.46	0.61	0.78	1.19	1.19	1.46	0.18	0.25	0.22	3.45	0.00	0.21	0.00

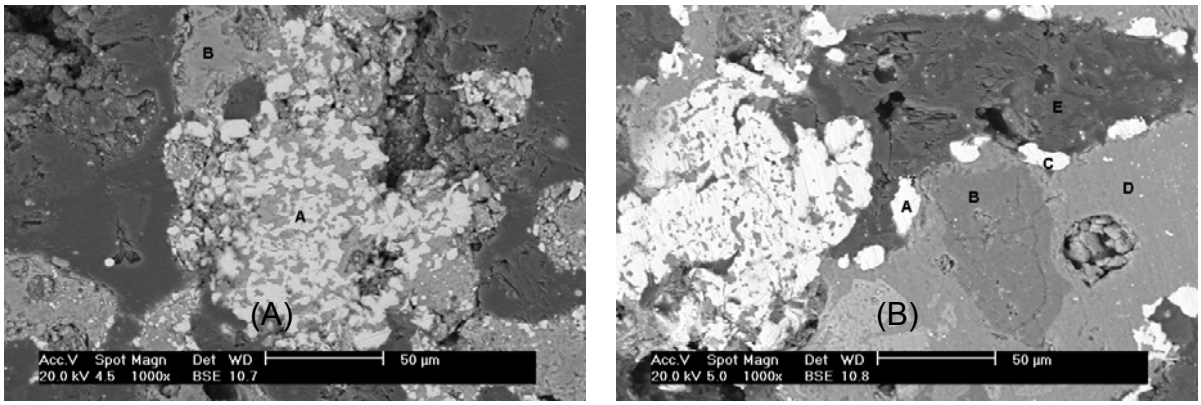

Figure 4 – Micrograph (SEM) of the self-reducing pellets submitted during 5 minutes at 1523K (A) and at 1573 (B). Reaction fractions around 45 and 50% , respectively.

Table 5.EDX of Figure 4-A

Phase	O	C	Mg	Al	Si	P	S	Ca	Cr	Mn	Fe	Co	Ni	Cu	Zn
A	0.00	29.89	0.00	0.26	0.65	0.67	0.25	0.00	0.40	0.39	66.26	0.00	0.32	0.53	0.40
B	14.43	0.00	0.00	6.88	29.88	1.69	0.92	0.34	0.50	1.56	37.32	4.43	0.68	0.53	0.84

Table 6.EDX of Figure 4-B

Phase	O	C	Al	Si	P	S	Ca	Cr	Mn	Fe	Co	Ni	Cu	Zn
A	0.00	0.60	0.54	0.88	1.20	0.49	0.15	0.30	0.32	92.75	0.00	2.10	0.39	0.28
B	26.74	0.00	1.30	65.55	0.75	0.17	0.23	0.27	0.28	4.71	0.00	0.00	0.00	0.00
C	0.00	0.00	0.57	0.68	0.77	0.31	0.15	0.31	0.37	92.00	1.45	2.37	0.72	0.30
D	19.19	0.00	8.16	35.83	1.30	0.70	1.47	0.75	3.19	27.91	0.51	0.34	0.22	0.43
E	2.43	89.94	0.22	0.38	0.51	1.33	0.15	0.24	0.27	3.14	0.35	0.41	0.31	0.32

In Figures 4A and 4B, it was observed a pronounced formation of metallic phase as well as small metallic particles scattered in the matrix. At temperature of 1573 a coalescence of metallic particles looks to start.

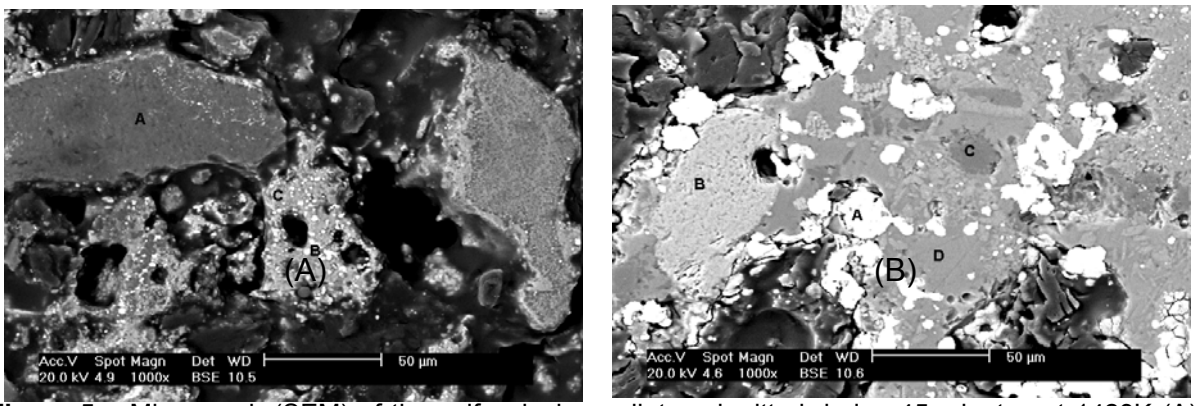

Figure 5 – Micrograph (SEM) of the self-reducing pellets submitted during 45 minutes at 1423K (A) and at 1473 (B). Reaction fractions around 50 and 60% , respectively

Table 7. EDX of Figure 5-A

Phase	O	C	Mg	Al	Si	P	S	Ca	Cr	Mn	Fe	Co	Ni	Cu
A	15,40	11.00	22.04	2.10	36.55	0.61	0.34	0.48	0.53	0.43	9.47	0.30	0.30	0.47
B	0.00	5.48	0.99	0.50	1.06	0.53	0.19	0.23	0.41	0.90	86.68	1.83	0.42	0.78

Table 8. EDX of Figure 5-B

Phase	O	C	Mg	Al	Si	P	S	Ca	Cr	Mn	Fe	Co	Ni	Cu
A	15.4	11.00	22.04	2.10	36.55	0.61	0.34	0.48	0.53	0.43	9.47	0.30	0.30	0.47
B	0.00	5.48	0.99	0.50	1.06	0.53	0.19	0.23	0.41	0.90	86.68	1.83	0.42	0.78
C	17.78	0.00	0.56	76.91	1.10	0.63	0.20	0.37	0.20	2.16	0.09	0.00	0.00	0.00
D	12.12	4.94	12.56	42.61	1.12	0.68	2.50	0.40	3.80	16.69	0.42	0.74	0.52	0.90

In Figure 5A, it was observed still a presence of original material grains and the formation of metallic from the easily reduced iron oxide particles (not silicates). Figure 5B shows the presence of some coalescent of metallic phase with tendency of spherical shape. The micrograph demonstrates the presence of many phases. The phase D is typically a “gangue” of the sludge, with high content of silicon oxide. Phase (B) is a chromite.

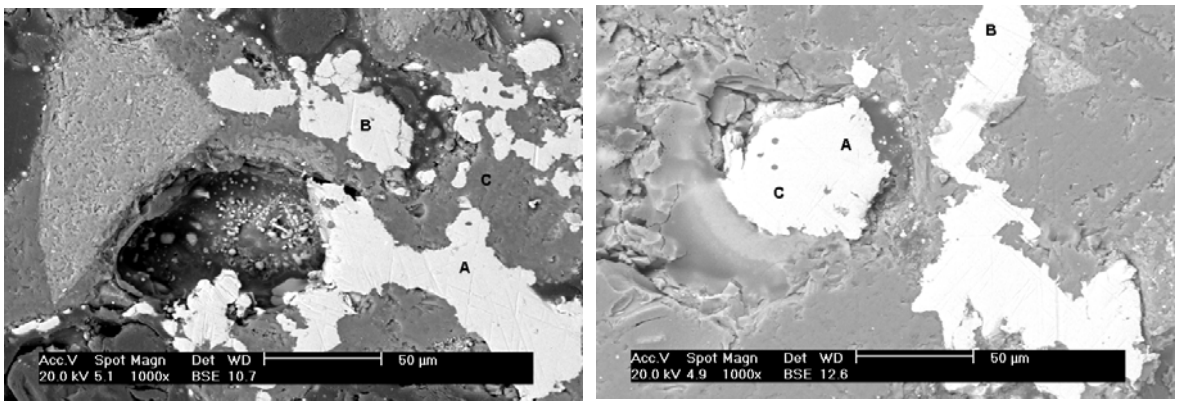

(A) (B)

Figure 6 – Micrograph (SEM) of the self-reducing pellets submitted during 45 minutes at 1523K (A) and at 1573 (B). Reaction fractions around 75 and 80% respectively

Table 9. EDX of Figure 6-A

Phase	O	C	Mg	Al	Si	P	S	Ca	Cr	Mn	Fe	Co	Ni	Cu	Zn
A	0.00	0.73	0.00	0.39	0.80	1.32	0.53	0.16	0.32	0.30	91.45	1.48	1.79	0.42	0.31
B	0.00	0.85	0.00	0.00	0.35	0.82	0.38	0.22	0.48	0.28	94.67	0.89	1.06	0.00	0.00
C	15.66	0.00	4.81	10.36	39.85	1.21	0.69	1.99	0.58	3.50	19.30	0.47	0.54	0.37	0.67

Table 10. EDX of Figure 6-B

Phase	C	Al	Si	P	S	Ca	Cr	Mn	Fe	Co	Ni	Cu	Zn
A	1.11	0.55	6.27	1.15	0.39	0.07	0.33	0.00	87.61	1.20	1.32	0.00	0.00
B	0.28	0.57	0.76	1.23	0.48	0.06	0.96	0.16	91.49	1.72	1.44	0.54	0.31
C	0.00	0.00	4.85	0.57	0.30	0.00	0.70	0.47	86.75	2.04	2.20	0.97	1.15

In the Figure 6A and 6B, it can be observed the coalescence of the metallic phase with dimensions higher than 50 μm. Even at high temperature the coalescence of the metallic phase was not complete. The high viscosity slag (high silica content) avoid good coalescence as can be seen by the presence of irregular shape of the metallic phase in the Figure 6-B (1573K, 45 minutes).

4 CONCLUSIONS

1. At the experimental condition two reactions control mechanisms were observed. At the beginning up to 10 minutes of reaction with the apparent activation energy of 86 kJ/mol which is probably controlled by heat transfer. The second step with higher activation energy (135kJ/mol) which is credited to be controlled by the diffusion in the solid state.
2. The maximum reaction fraction reached for the experimental conditions was 80%.
3. It can be observed that in the 5 minutes experiment, for all temperatures, the growth of the metallic phase was incipient. Even at higher temperature (1573K) and for longer time (45minutes) the coalescence was not complete.
4. The influence of temperature was as expected. Higher temperature presented higher reaction fraction at same time of reduction.

Acknowledgements

The authors would like to thank to CAPES and FAPESP for their financial support for the development of this scientific research as well as the University of São Paulo (USP).

REFERENCES

1 C. TAKANO; CAPOCCHI, J.D.; NASCIMENTO, R.C.; MOURÃO, M.B; LENZ, G.; DOS SANTOS, D.M,; A reciclagem de resíduos siderúrgicos solidos. Seminario Nacional sobre Reuso/Reciclagem de Residuos Sólidos industrias secretaria do Meio Ambiente SP. 28-31/8/2000
2 NASCIMENTO, R.C. Uma análise microestructural sobre pelotas auto-redutoras. Teses de Doutorado EPUSP, 1994.
3 STROIHMEIER G.;BONESTELL,J.E. Steelworks residues and the Wales kiln treatment of electric furnace dust. Iron and Steel Engineer, v.73, n.4, pp. 87-90, 1996.
4 SOBRINHO, P. J.; TENORIO, J.A. Processos para o aproveitamento de poeiras geradas durante a fabricação de aço.
5 GOICOECHEA, T.; Gandia N. Recuperación de residuos de cinc y plomo en la nueva planta del norte. Cia. IV Reunión de la comisión Técnica de Minerales de Hierro. CENIM. Madrid, 1986.
6 LÓPEZ, F. A.; MEDINA, F.; MEDINA, J. Tratamientos de polvos de acería eléctrica mediante procesos hidrometalurgicos y reducción carbotermica. Revista de Metalurgica, Madrid. Vol. 26 (1), 1990, pp. 1-68.
7 Seaton, C; Structural changes occurring during reduction of hematite and magnetite pellets containing coal char, ISIJ, 23, 1983, PP. 490.

8 MOURÃO, M.B.; CAPOCCHI, J.D.T.; Rate of reduction of iron oxide in carbon-bearing pellets. Mineral Processing and Extractive Metallurgy, 105, Sep-Dec, 1996, pp 190.
9 MOURÃO, M.B. Análise do processo de redução de minério de ferro por carbono na forma de pelotas auto-redutoras. Teses de Doutorado EPUSP, 1988.
10 BURKIN A. R. Extractive Metallurgy of Nickel, 1987 by the Society of Chemical Industry.
11 NEIRA J. V.; MOURÃO M.B; TAKANO C. Caracterización de residuos de La producción de níquel. Agosto. 2008 congreso nacional de minería. Lima –Peru.
12 SANTOS D.M.;MOURÃO M.B; TAKANO C. Recuperação do ferro das lamas de aciaria na forma de pelotas auto-redutoras:comparação entre procesos de auto-redução e fusão redução.XXXIII Seminari de Fusão, Refino e Solidificação-ABM, 2002.
13 NASCIMENTO, R.C; MOURÃO, M.B.; CAPOCCHI, J.D.T.; kinetics and catastrophic swelling during reduction of ore in carbon bearing pellets. Ironmaking and Steelmaking, 199, Vol 26 No. 3 pp.182-186.
14 Seaton, C; Structural changes occurring during reduction of hematite ande magnetite pellets containing coal char, ISIJ, 23, 1983, PP. 490.
15 ABRAHAN, M.C.; GHOSH,A.; Kinetics of reduction of iron oxide by carbon. Ironmaking and Steelmaking, 1, 1979, pp. 14.